NUCLEAR PHYSICS

Measurement of the neutron lifetime using a magneto-gravitational trap and in situ detection

R. W. Pattie Jr.,[1] N. B. Callahan,[2] C. Cude-Woods,[1,3] E. R. Adamek,[2] L. J. Broussard,[4] S. M. Clayton,[1] S. A. Currie,[1] E. B. Dees,[3] X. Ding,[5] E. M. Engel,[6] D. E. Fellers,[1] W. Fox,[2] P. Geltenbort,[7] K. P. Hickerson,[8] M. A. Hoffbauer,[1] A. T. Holley,[9] A. Komives,[10] C.-Y. Liu,[2] S. W. T. MacDonald,[1] M. Makela,[1] C. L. Morris,[1] J. D. Ortiz,[1] J. Ramsey,[1] D. J. Salvat,[11] A. Saunders,[1]* S. J. Seestrom,[1]† E. I. Sharapov,[12] S. K. Sjue,[1] Z. Tang,[1] J. Vanderwerp,[2] B. Vogelaar,[5] P. L. Walstrom,[1] Z. Wang,[1] W. Wei,[1] H. L. Weaver,[1] J. W. Wexler,[3] T. L. Womack,[1] A. R. Young,[3] B. A. Zeck[1,3]

The precise value of the mean neutron lifetime, τ_n, plays an important role in nuclear and particle physics and cosmology. It is used to predict the ratio of protons to helium atoms in the primordial universe and to search for physics beyond the Standard Model of particle physics. We eliminated loss mechanisms present in previous trap experiments by levitating polarized ultracold neutrons above the surface of an asymmetric storage trap using a repulsive magnetic field gradient so that the stored neutrons do not interact with material trap walls. As a result of this approach and the use of an in situ neutron detector, the lifetime reported here [877.7 ± 0.7 (stat) +0.4/−0.2 (sys) seconds] does not require corrections larger than the quoted uncertainties.

Measurement of free neutron decay to a proton, electron, and antineutrino, $n \rightarrow p + e^- + \bar{\nu}_e$, provides information about the fundamental parameters of the charged weak current of the nucleon and constrains many extensions to the Standard Model at and above the tera–electron volt scale. Knowledge of the mean neutron lifetime, τ_n, to an accuracy of better than 1 s is necessary to improve big-bang nucleosynthesis predictions of elemental abundances (*1*) and to search for physics beyond the Standard Model of nuclear and particle physics (*2*).

The neutron lifetime has recently been measured with two different techniques (*3*, *4*): counting the surviving ultracold neutrons after storage in material-walled traps, with a most precise result of 878.5 ± 0.8 s (*5*), and counting the number of decay products emerging from a passing beam of cold neutrons, with a result of 887.7 ± 2.2 s (*6*). The results of these techniques disagree by 9.2 s, or 3.9 standard deviations.

Our experiment was designed to reduce systematic uncertainties by using ultracold neutrons (UCNs) trapped in a storage volume closed by magnetic fields on the bottom and sides and by gravity on top, as previously demonstrated in (*7*, *8*). In this work, we have used an asymmetric trap to reduce the population of long-lived closed neutron orbits with kinetic energies over the storable energy threshold in the trap (*9*, *10*). We have also introduced in situ detection of the surviving neutrons to eliminate uncertainties associated with transporting the neutrons to an ex situ detector. Recent storage experiments used storage traps with variable volumes to extrapolate to infinite volume in an attempt to reduce uncertainties associated with losses of neutrons caused by interactions with the material walls (*5*, *11*–*15*). Our experiment had no detectable losses of neutrons caused by interactions with the magnetic and gravitational "walls" of the trap and thus required no extrapolation. In addition, we used a number of techniques to diagnose and eliminate effects of quasi-trapped neutrons. These neutrons have kinetic energies above the trapping potential but nevertheless can reside in the trap in quasi-stable orbits for hundreds of seconds, skewing the long storage time measurements.

Ultracold neutron delivery, storage, and measurement protocol

The experimental technique was described in detail in (*16*) and is summarized here. The experimental apparatus is shown in Fig. 1. UCNs were supplied by the west beam line of the Los Alamos Neutron Science Center UCN facility (*17*–*19*). The UCN flux was monitored by normalization detectors (*20*) that sampled the flux through small aperture holes in the beam guide. The neutrons were polarized with a 6-T solenoid magnet that transmitted only neutrons in the "high-field-seeking" spin state. An adiabatic fast passage spin flipper changed the spin state of the neutrons to low-field-seeking with ~90% efficiency by using an applied magnetic field of 14 mT and an oscillating radio-frequency field of 372 kHz. Another normalization detector mounted above the storage height of the neutron trap monitored the UCN flux just before the entrance to the trap. The neutrons reaching this detector height had too much kinetic energy to be confined by gravity in the magnetic trap. The flux at each detector was monitored throughout the filling period in order to determine the relative normalization of the number of neutrons entering the trap in each storage run. Neutrons filled the trap through a movable magnetic door located at the bottom of the apparatus.

The trap was constructed of a Halbach array of permanent magnets in which the magnetization of each row of permanent magnets was rotated 90° relative to its neighbors. Each NdFeB magnet was 2.54 cm by 5.08 cm by 1.27 cm, with a surface field of ~1.0 T. The magnets were installed along the surface of two intersecting tori, one with a major radius of 100 cm and a minor radius of 50 cm, the other with the radii interchanged and cut off at a height of 50 cm from the bottom of the trap, thus forming an asymmetric trap with a trapping potential of ~50 neV (corresponding to neutron temperature $\lesssim$0.58 mK) and a fiducial volume of 420 liters. An additional externally applied holding field of up to 10 mT, approximately perpendicular to the Halbach field, was used to maintain the neutron polarization during the storage period. The performance of the trap was described in (*10*).

At the end of the 150-s filling period, the 800-MeV proton beam that produced the UCN was turned off so as to reduce backgrounds, and the loading trap door and other valves in the UCN beam pipe were closed, preventing further neutrons from reaching the apparatus. A cleaning period followed, designed to eliminate any neutrons in the trap with kinetic energy sufficient to escape the trap. A horizontal sheet of polyethylene, called the "cleaner," removed neutrons with sufficient kinetic energy to reach its height via absorption or thermal upscattering. During the filling and cleaning periods, the cleaner was positioned 38 cm above the bottom of the trap, or 12 cm below the nominal open top of the trap. The cleaner covered approximately one half of the horizontal surface of the trap at its mounted height [~0.86 m^2, to be compared with the 0.23 m^2 horizontal cleaner used in the work of (*16*)], so that every neutron capable of reaching it did so quickly within a few tens of seconds after entering the trap. A second "active" cleaner, with 28% of the area of the primary cleaner, was mounted on the downstream side of the trap in the same plane as the primary cleaner. This second cleaner used ^{10}B-coated ZnS:Ag as the UCN absorber (*20*) and was

[1]Los Alamos National Laboratory, Los Alamos, NM 87545, USA. [2]Center for Exploration of Energy and Matter and Department of Physics, Indiana University, Bloomington, IN 47408, USA. [3]Triangle Universities Nuclear Laboratory and North Carolina State University, Raleigh, NC 27695, USA. [4]Oak Ridge National Laboratory, Oak Ridge, TN 37831, USA. [5]Department of Physics, Virginia Polytechnic Institute and State University, Blacksburg, VA 24061, USA. [6]West Point Military Academy, West Point, NY 10996, USA. [7]Institut Laue-Langevin, Grenoble, France. [8]Kellogg Radiation Laboratory, California Institute of Technology, Pasadena, CA 91125, USA. [9]Department of Physics, Tennessee Technological University, Cookeville, TN 38505, USA. [10]Department of Physics and Astronomy, DePauw University, Greencastle, IN 46135-0037, USA. [11]Department of Physics, University of Washington, Seattle, WA 98195-1560, USA. [12]Joint Institute for Nuclear Research, Dubna, Moscow region 141980, Russia.
***Corresponding author. Email: asaunders@lanl.gov**
†Present address: Sandia National Laboratories, Albuquerque, NM 87185, USA.

Downloaded from http://science.sciencemag.org/ on May 10, 2018

observed with an array of photomultiplier tubes (PMTs), allowing the UCN density in the plane of the cleaners to be continuously monitored. At the conclusion of the cleaning period, 50 to 300 s for the data presented here, both cleaners were raised 5 cm in order to stop further interactions; at this point, the storage period began. The neutrons were stored for times typically ranging from 10 to 1400 s, chosen to optimize statistical reach in a given experimental running time while still permitting systematic studies.

At the end of the storage period, a UCN detector consisting of a vertical poly(methyl methacrylate) (PMMA) paddle coated on both sides with ZnS:Ag and ^{10}B, with a total active surface area of 750 cm^2 per side (~21% of the 3450 cm^2 area of the midplane of the trap), was lowered into the center of the trap. The detector could be lowered in multiple steps and, at its lowest position, reached to within 1 cm of the bottom of the trap. Because the detector could only access the fraction of UCNs that had sufficient energy to reach the height of each step, this permitted rate-dependent uncertainties to be studied by controlling the counting rate and also enabled the exploration of different neutron energy– and phase space–dependent systematic effects. The detector removed (or "unloaded") the surviving stored neutrons from the trap with a time constant of ~8 s. At the conclusion of the counting period (typically 100 to 300 s in length, or many 8-s mean draining times), the detector was left in the trap to count background rates with no neutrons in the trap for typically 150 s. The absolute efficiency of the detector, previously reported to be 96% (*16*), and those of the upstream monitor detectors cancel in the ratios used to extract the lifetime in this experiment.

Each neutron absorbed on the detector's boron layer generated a burst of scintillation photons in the ZnS:Ag scintillator that were converted and conducted from the transparent PMMA backing plate to a pair of photomultiplier tubes by an array of 2-mm-spaced wavelength shifting fibers. The photons in each PMT were individually counted with an 800-ps precision time stamp by an input channel of the same multichannel scaler (MCS) (*21*) that counted the output pulses from the normalization monitors.

In a typical measurement cycle, a pair of runs were performed, one with a nominal short storage time of 20 s and one with a nominal long storage time of 1020 s, each with ~2.5 × 10^4 neutrons in the trap at the beginning of the storage period. A total of 332 pairs of long and short runs were analyzed for the results in this paper, in five different running configurations. The different run conditions varied the cleaning time, the number of steps in which the detector was lowered into the trap, and the magnitude of the applied neutron polarization holding field. The five run conditions are listed in Table 1.

Shown in Fig. 2, A and B, are a "nine-step" and "three-step," respectively, unloading curve for a short and long storage time, summed over all the cycles in the respective run condition. An unloading curve is a plot of the instantaneous rate of neutron detection in the UCN detector, during the counting period after the UCN storage time. In each case, the first, highest detector step placed the bottom edge of the detector at the cleaning height so that no stored neutrons had sufficient energy to reach the 132 cm^2 of active area that extended below the position of the raised cleaners. No neutrons above background were detected in this step, putting constraints on systematic uncertainties caused by insufficient cleaning of high-energy neutrons and heating of neutrons by vibrations, to be described later: Only eight peaks are visible in the nine-step unloading curve and two in the three-step curve. The absolute start time of the

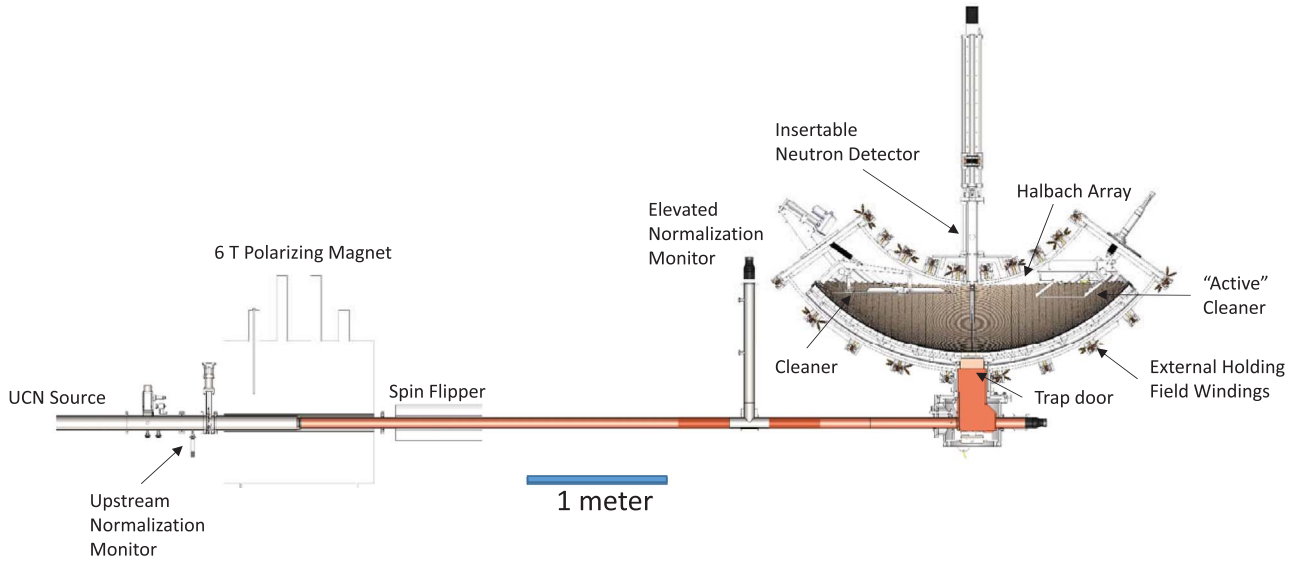

Fig. 1. Layout of the UCN beam line and trap used for these measurements.

Table 1. The five running conditions analyzed in this paper. "Detector steps" is the number of discrete counting positions as the neutron detector was lowered to the bottom of the trap; "Cleaning time" is the length of cleaning period from the closing of the neutron loading trap door to the raising of the cleaner; "Holding field" is the minimum strength of the externally applied polarization holding field in the trap; and "Run pairs" is the number of long-short run pairs acquired for this configuration, all with roughly equal numbers of initially loaded neutrons.

Run configuration	Detector steps	Cleaning time (s)	Holding field (mT)	Run pairs
A	1	200	6.8	79
B	9	200	6.8	66
C	9	300	6.8	70
D	3	50	6.8	60
E	3	50	3.4	57

Downloaded from http://science.sciencemag.org/ on May 10, 2018

long storage curve was adjusted in each plot by the difference between the nominal long and short storage times, to allow visual comparison of the curves.

The data were blinded by adjusting the nominal storage times (along with all the MCS time stamps in a blinded run) by a factor hidden from those analyzing the data, with the result that τ_n extracted from the blinded data differed from the actually measured value by a random offset of up to ±15 s.

Extracting the neutron lifetime

The expected number of surviving neutrons after storing an initial number N_0 of neutrons in the trap for a time t is $N_{surv} = N_0 e^{-t/\tau_{meas}}$, where τ_{meas} is the mean measured survival time of the trapped neutrons. The measured loss rate is the sum of the loss rate caused by neutron decay and all other sources of loss from the trap, such as losses caused by interactions with the walls, depolarization of neutrons during storage, thermal upscattering of neutrons from residual gas in the trap, or other sources of loss: $1/\tau_{meas} = 1/\tau_n + 1/\tau_{loss}$.

The number of surviving neutrons was estimated from the raw data, consisting of a string of time-stamped photon events from the two in situ detector PMTs, using two different techniques. The first method required a coincidence between photons from each of the two PMTs to identify a neutron. Coincidences were identified during a 50-ns window, followed by an above-threshold number of photons in a variable integration window of several microseconds. The threshold was determined by the number and arrival time of previously identified neutrons in the data stream. Identification of new neutrons was disabled during the integration window, creating a rate-dependent but calibrated software dead time for each counting bin. The integration window was extended in 1-μs steps as long as photon events continued to arrive, in order to maximize neutron identification efficiency while minimizing software dead time. The second method used individual photons, or "singles" data. Each individual photon was treated as an independent event, with no attempt made to identify the neutron responsible for each individual photon.

The normalized total signals of the surviving UCN populations, or yields, were calculated for each run by summing the counts measured in all detector positions, subtracting experimental backgrounds, and dividing by the relative number of neutrons loaded into the trap. The background at long holding times was on the order of 0.3% of signal for coincidence counting and 15% for singles counting. The raw numbers of neutrons (coincidence) or photons (singles) were corrected for dead time [(*22*), section 1]. The relative number of neutrons loaded into the trap was determined from the counts in the elevated normalization monitor [Fig. 1 and (*22*), section 2], exponentially weighted by the measured loading time constant of the trap (60 to 70 s). Spectral variations in the incident neutron flux were assessed by taking the ratio of the number of counts in the elevated normalization detector to the number in the upstream, beam-height normalization detector. The first-order correction to the normalization, as much as 10% over a period of 100 hours, was determined by minimizing the variance of neutron yields of short-storage runs only. Alternating long and short storage time runs reduced the effect of this correction on the lifetime uncertainty to negligible levels.

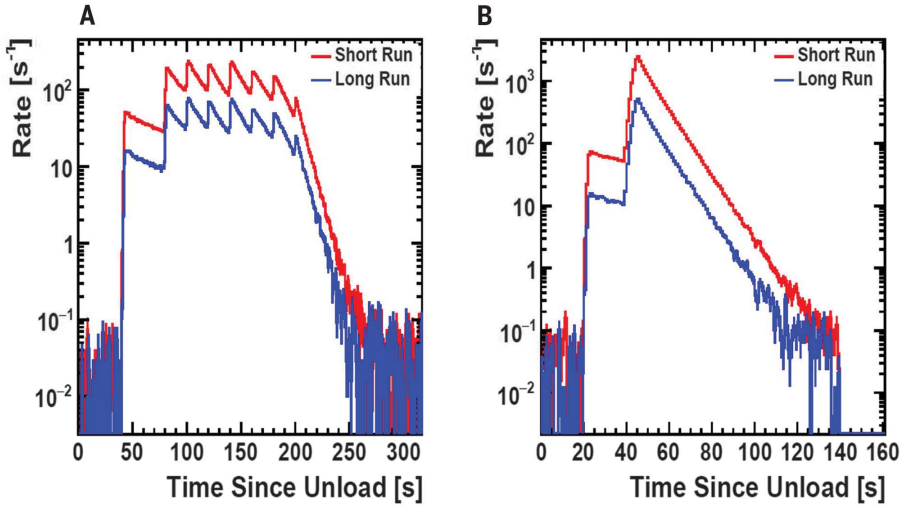

Fig. 2. Unloading time distributions. (**A** and **B**) The combined rates of the neutron signals and backgrounds for a (A) nine-step configuration and (B) three-step configuration. The times have been shifted to align the short storage time (red) and long storage time (blue) distributions.

The neutron lifetime and uncertainty were calculated from pairs of short and long storage time yields using

$$R_i \equiv \frac{Y_{is}}{Y_{il}} \quad (1)$$

$$\tau_{n,i} = \frac{(\bar{t}_l - \bar{t}_s)}{\ln(R_i)} \quad (2)$$

and

$$\Delta\tau_{n,i} = \frac{(\bar{t}_l - \bar{t}_s)}{\ln(R_i)^2}\frac{\Delta R_i}{R_i} \quad (3)$$

where the subscripts l and s denote long and short storage times, $\bar{t}$ is the mean neutron detection time during the counting period, Ys are the yields, τ_n is the lifetime, the Δs indicate uncertainties, and the subscript i denotes the individual run pairs. Uncertainties were calculated by using Poisson statistics for the UCN yields, including the statistics of the exponentially weighted elevated normalization monitor counts. The statistical uncertainty in the photon singles yields were obtained from the coincidence data and by analyzing the variance in the singles-extracted lifetimes, and both approaches produced consistent results.

Average lifetimes were calculated for each of the five run configurations in three ways. First, the average long and short yields across a run configuration were calculated and assigned uncertainties as the standard deviation of the individual yields divided by $\sqrt{N}$, where N is the number of individual run pair yields. The lifetimes and uncertainties were calculated from the average values by using Eqs. 1 to 3. The second method determined the lifetime from a weighted average of the lifetimes calculated from each individual run pair. In this case, the uncertainty was calculated from the weighted average of individual run pair uncertainties and multiplied by the square root of the reduced χ^2 to account for any remaining nonstatistical variation in the data set caused by smaller systematic effects such as higher-order time or spectral variations in the loaded neutrons. The third method was identical to the second, except that an unweighted average was used to compute the average lifetime.

Systematic uncertainties

The total systematic uncertainty in these results were estimated to be 0.28 s. The major sources of systematic uncertainties in these results are listed in Table 2.

The only correction applied to the central value of the lifetime was due to thermal upscattering of UCN from individual interactions of UCN, with residual gas particles in the trap during the storage period. Because the cross section for neutron scattering off of residual gas molecules is inversely proportional to the neutron velocity, the residual gas pressure, molecular make up, and interaction cross sections could be combined to extract a neutron loss lifetime, independent of neutron velocity, caused by this upscattering effect

$$1/\tau_{upscatter} = \sigma_{upscatter} v_n N_{gas} \quad (4)$$

Downloaded from http://science.sciencemag.org/ on May 10, 2018

$$\sigma_{\text{upscatter}} = \sigma_{\text{free}}\bar{v}_{\text{gas}} \Big/ v_n \quad (5)$$

$$1\Big/\tau_{\text{upscatter}} = \sigma_{\text{free}}\bar{v}_{\text{gas}}N_{\text{gas}} \quad (6)$$

where $\tau_{\text{upscatter}}$ is the loss lifetime because of this upscatter effect, $\sigma_{\text{upscatter}}$ is the cross section for upscattering of neutrons from residual gas molecules, σ_{free} is the velocity-independent neutron-gas interaction cross section, $\bar{v}_{\text{gas}}$ is the mean velocity of the gas molecules, and N_{gas} is the number density of gas molecules, proportional to the pressure. Equations 4 to 6 apply to a single gas species but could easily be summed over all gases in the storage volume. Two calibrated cold cathode gauges located above the midplane of the trap were used to measure the residual gas pressure (typically 6×10^{-7} torr), and a residual gas analyzer was used to measure the mass spectrum of the residual gas. From these measurements and the measured UCN cross sections from (*23*, *24*), we calculated the velocity-independent UCN lifetime ($\tau_{\text{upscatter}}$), which is caused by losses on the residual gas in the trap, using Eqs. 4 to 6. The loss rate from this lifetime was then subtracted from the measured neutron loss rate to yield the neutron decay loss rate, for a correction to the measured lifetime of 0.16 s with an uncertainty of 0.03 s [(*22*), section 3].

The systematic uncertainty caused by possible depolarization of neutrons during the storage period was assessed by measuring the neutron lifetime while varying the magnitude of the applied polarization holding field [(*22*), section 4]. High-precision lifetime measurements were made at holding field strengths of 6.8 and 3.4 mT, and lower-precision measurements at smaller fields down to 0 mT applied field. The resulting lifetimes were fitted by using a power law suggested in (*25*) from calculations of depolarization in the present trap geometry: $\frac{1}{\tau} = \frac{1}{\tau_n} + \frac{B_{\perp 0}^3}{B_\perp^2 \tau_{DP}}$, where $B_\perp$ is the holding field, $B_{\perp 0}$ is the full holding field, τ is the measured storage lifetime, τ_n is the neutron decay lifetime, and τ_{DP} is the loss lifetime due to depolarization. The result of the fit yielded a loss lifetime owing to depolarization of $\tau_{DP} = 1.1 \times 10^7$ s (with 1σ uncertainty bounds of 6.0×10^6 and 5.5×10^7 s) for an uncertainty on the measured neutron lifetime of 0.07 s. The 6.8 and 3.4 mT measurements showed no variation outside of statistics.

Neutrons can be heated by, for example, many small interactions with the vibrational motion of the UCN trap's magnetic field, slowly gaining enough energy to exceed the trap potential and escape from the trap during the long storage period. A limit on the uncertainty due to this effect was determined by looking for neutrons moving into the highest neutron detector position (38 cm above the bottom of the trap, or equal in height to the lowered cleaner), in run configurations B to E during the long storage time (Table 1).

The detector's ability to count these very low-energy UCNs (<5 neV kinetic energy at the top of their orbits in the trap) was verified by loading the trap with the cleaners and the neutron detector in their raised position. The counting curve from the active cleaner was observed to fall to its background rate in ~10 s and was constant thereafter, indicating that neutrons were efficiently cleaned to the height of the raised cleaners (43 cm above the bottom of the trap). The neutron detector was then lowered to the upper counting position and was observed to count UCN with sufficient energy to reach heights between 38 and 43 cm with a time constant of 260 s [(*22*), section 5]. Although only the lowest 5 cm of the detector was exposed below the raised cleaners during the first step of a nominal lifetime run, characterization of the neutron detector with a Gd-148 α particle source showed an approximately uniform optical response across the entire active area of the detector. In addition, heated UCN gain energy slowly and so have multiple opportunities to be captured by the detector before acquiring sufficient energy to reach the position of the raised cleaners. In estimating the cleaning and heating systematic uncertainties, a conservative factor of 20 was applied to account for neutrons that were not detected during the 20-s first-position counting time used for lifetime running.

The number of neutrons observed in the highest counting position was consistent with background in the long storage time runs. The systematic uncertainty due to heating was determined by the uncertainty of the yield calculated by using only the counts observed in the highest position. On the basis of this analysis, we put a 1σ limit on the lifetime uncertainty because of neutron heating of 0.23 s.

Similarly, insufficient cleaning of neutrons with energy above the trapping energy would result in an artificial excess of counts after the short storage time that could be lost over the long storage time. An analysis of excess neutrons in the highest counting position in the short storage time runs, which is also consistent with zero neutrons above background, allowed us to put a limit of 0.06 s on the uncertainty in the measured lifetime because of insufficient cleaning.

In the single-photon counting analysis method, a hardware dead time was caused by the 10-ns dead time of the discriminator used to detect the individual photons. The uncertainty due to correcting for this rate-dependent effect was set to 20% of the correction on each run, for a total uncertainty on the extracted lifetime of 0.04 s.

Phase space evolution can cause a possible change in effective detector efficiency between the short and long storage time runs caused by evolution of the neutron population in the trap between regions of phase space with different degrees of access to the detector location. Any effect of phase space evolution on the measured lifetime would cause a variation in the relative number of neutrons in the peaks corresponding to the different counting steps between the short

Table 2. Systematic uncertainties.

Effect	Upper bound (s)	Direction	Method of evaluation
Depolarization	0.07	+	Varied external holding field
Microphonic heating	0.24	+	Detector for heated neutrons
Insufficient cleaning	0.07	+	Detector for uncleaned neutrons
Dead time/pileup	0.04	±	Known hardware dead time
Phase space evolution	0.10	±	Measured neutron arrival time
Residual gas interactions	0.03	±	Measured gas cross sections and pressure
Background shifts	<0.01	±	Measured background as function of detector position
Total	0.28		(uncorrelated sum)

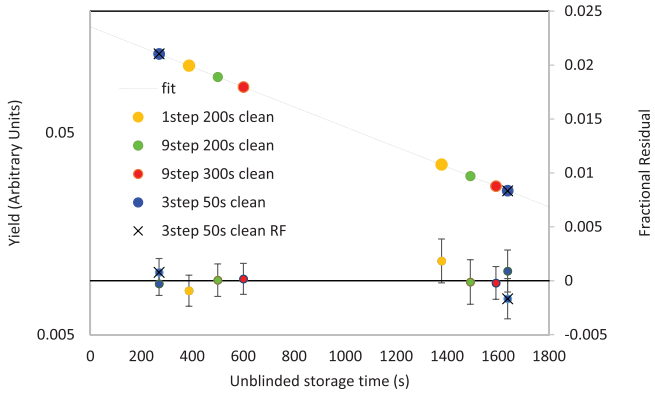

Fig. 3. Yields as a function of storage time. The yields are shown relative to the start of filling for each of the running conditions. The relative normalization of the data sets has been adjusted to account for the different running conditions. The dashed line shows an exponential fit to the yields. The fractional residuals, or differences between the yields and the fitted curve, are plotted against the right axis. RF denotes the use of a reduced polarization holding field strength of 3.4 mT instead of 6.8 mT.

Downloaded from http://science.sciencemag.org/ on May 10, 2018

and long storage time runs; therefore, a limit on this effect was estimated by calculating the statistical uncertainty of the centroid of the unloading curve for the nine-step measurements and was found to be 0.10 s [(*22*), section 6]. The effect was smaller for the one- and three-step measurements. A cross check was made for the presence of neutron population phase space evolution between the short and long storage periods by comparing the number of counts in each of the three or nine separate detector steps; the variation in these ratios was consistent with statistical fluctuations.

Results

As a final check for nonexponential behavior in the data, we performed a global fit to the yields of the long and short storage time measurements (Fig. 3). The unblinded measured neutron lifetime extracted from this fit was 877.6 ± 0.7 s, with a χ^2/df of 0.7. After correction for gas upscattering, the final unblinded measured mean neutron lifetime was 877.7 ± 0.7 (stat) +0.4/−0.2 (sys) s. The coincidence and the singles analysis methods described above yielded the same results. Three independent analyses were conducted and compared before unblinding. These analyses agreed to within 0.2 s. The central value of the result presented here is the average of the three results, the statistical uncertainty is the average of those from the three analyses, and the systematic uncertainty is that from Table 2 added in quadrature with an additional 0.2 s to account for the differences between the analysis techniques. Because the total uncertainty of this result is dominated by statistical uncertainty, and because the leading systematic uncertainties appear to be statistically driven and thus reducible with further study, we expect to ultimately reach a total uncertainty well below 0.5 s in future data runs using this apparatus.

The nonblinded data set presented in (*16*) was combined with a blinded systematics study data set, which had a statistical accuracy of $\Delta\tau_n$ = 1 s, to develop techniques to correct for incomplete cleaning of quasi-bound neutrons and to identify improvements to the trap-cleaning procedure. These improvements were implemented before acquiring the data discussed in this paper. The systematics study data were unblinded (based on two independent analyses) at the same time as the data presented here and produced a consistent result for τ_n. This data set was not included in the neutron lifetime result presented here.

The result presented here does not require corrections to the measured lifetime that are larger than the quoted uncertainties. This result agrees with the previous best measurement of the lifetime for neutron decay by using UCNs stored in a material trap and disagrees with the lifetime for neutron β-decay determined by using the beam technique.

REFERENCES AND NOTES

1. R. H. Cyburt, B. D. Fields, K. A. Olive, T.-H. Yeh, *Rev. Mod. Phys.* **88**, 015004 (2016).
2. W. J. Marciano, *Phys. Procedia* **51**, 19–24 (2014).
3. F. E. Wietfeldt, G. L. Greene, *Rev. Mod. Phys.* **83**, 1173–1192 (2011).
4. A. R. Young *et al.*, *J. Phys. G Nucl. Part. Phys.* **41**, 114007 (2014).
5. A. Serebrov *et al.*, *Phys. Rev. C Nucl. Phys.* **78**, 035505 (2008).
6. A. T. Yue *et al.*, *Phys. Rev. Lett.* **111**, 222501 (2013).
7. V. Ezhov *et al.*, *Nucl. Instrum. Methods Phys. Res. A* **611**, 167–170 (2009).
8. V. Ezhov *et al.*, arXiv:1412.7434 [nucl-ex] (23 December 2014).
9. P. Walstrom, J. D. Bowman, S. I. Penttila, C. Morris, A. Saunders, *Nucl. Instrum. Methods Phys. Res. A* **599**, 82–92 (2009).
10. D. J. Salvat *et al.*, *Phys. Rev. C Nucl. Phys.* **89**, 052501 (2014).
11. S. Arzumanov *et al.*, *Phys. Lett. B* **745**, 79–89 (2015).
12. A. Steyerl, J. M. Pendlebury, C. Kaufman, S. S. Malik, A. M. Desai, *Phys. Rev. C Nucl. Phys.* **85**, 065503 (2012).
13. A. Pichlmaier, V. Varlamov, K. Schreckenbach, P. Geltenbort, *Phys. Lett. B* **693**, 221–226 (2010).
14. J. Byrne *et al.*, *Europhys. Lett.* **33**, 187–192 (1996).
15. W. Mampe *et al.*, *JETP Lett.* **57**, 82 (1993).
16. C. L. Morris *et al.*, *Rev. Sci. Instrum.* **88**, 053508 (2017).
17. A. Saunders *et al.*, *Phys. Lett. B* **593**, 55–60 (2004).
18. A. Saunders *et al.*, *Rev. Sci. Instrum.* **84**, 013304 (2013).
19. T. M. Ito *et al.*, *Phys. Rev. C* **97**, 012501R (2018).
20. Z. Wang *et al.*, *Nucl. Instrum. Methods Phys. Res. A* **798**, 30–35 (2015).
21. FastCom, Model MCS6A, 64 Bit 5/(6) input 100 ps Multistop TDC, Multiscaler, Time-Of-Flight (2016); www.fastcomtec.com/fwww/datashee/photon/mcs6.pdf.
22. Supplementary text is provided as supplementary materials.
23. S. J. Seestrom *et al.*, *Phys. Rev. C Nucl. Phys.* **92**, 065501 (2015).
24. S. J. Seestrom *et al.*, *Phys. Rev. C Nucl. Phys.* **95**, 015501 (2017).
25. A. Steyerl, K. K. H. Leung, C. Kaufman, G. Müller, S. S. Malik, *Phys. Rev. C Nucl. Phys.* **95**, 035502 (2017).

ACKNOWLEDGMENTS

The authors thank the staff of LANSCE for their diligent efforts to develop the diagnostics and new techniques required to provide the proton beam for this experiment. **Funding:** This work was supported by the Los Alamos Laboratory Directed Research and Development (LDRD) office (no. 20140568DR), the LDRD Program of Oak Ridge National Laboratory, managed by UT-Battelle (no. 8215), the National Science Foundation (nos. 130692, 1307426, 161454, 1306997, and 1553861), NIST Precision Measurement Grant, IU Center for Space Time Symmetries (IUCSS), the LANSCE Rosen Scholarship program, and U.S. DOE Low Energy Nuclear Physics (nos. DE-FG02-97ER41042 and DE-AC05-00OR22725). **Competing interests:** None declared. **Author contributions:** Experiment design was performed by R.W.P., N.B.C., C.C.-W., E.R.A., S.M.C., W.F., P.G., K.P.H., A.T.H., A.K., C.-Y.L., M.M., C.L.M., J.R., D.J.S., A.S., S.J.S., E.I.S., S.K.S., J.V., P.L.W., and A.R.Y.; experiment construction was performed by R.W.P., N.B.C., C.C.-W., E.R.A., S.M.C., S.A.C., X.D., A.T.H., C.-Y.L., S.W.T.M., M.M., C.L.M., J.D.O., D.J.S., A.S., J.V., B.V., W.W., T.L.W., A.R.Y., and B.A.Z.; detector research and development was performed by R.W.P., C.C.-W., E.R.A., D.E.F., M.A.H., M.M., C.L.M., J.D.O., J.R., D.J.S., E.I.S., and Z.W.; data acquisition was performed by R.W.P., N.B.C., C.C.-W., E.R.A., L.J.B., S.M.C., E.B.D., E.M.E., D.E.F., P.G., K.P.H., A.T.H., A.K., C.-Y.L., M.M., C.L.M., J.D.O., D.J.S., A.S., S.J.S., S.K.S., Z.T., P.L.W., W.W., H.L.W., J.W.W., A.R.Y., and B.A.Z.; and data analysis was performed by R.W.P., N.B.C., C.C.-W., E.R.A., S.M.C., A.T.H., C.-Y.L., C.L.M., D.J.S., and S.J.S. **Data and materials availability:** The data shown in this paper are available as part of the supplementary materials. The raw data that underlie these results are curated at Los Alamos National Laboratory and are available upon request from the corresponding author.

SUPPLEMENTARY MATERIALS

www.sciencemag.org/content/360/6389/627/suppl/DC1
Supplementary Text
Figs. S1 to S9
Data File S1

2 June 2017; accepted 13 March 2018
Published online 6 May 2018
10.1126/science.aan8895

Downloaded from http://science.sciencemag.org/ on May 10, 2018

Science

Measurement of the neutron lifetime using a magneto-gravitational trap and in situ detection

R. W. Pattie Jr., N. B. Callahan, C. Cude-Woods, E. R. Adamek, L. J. Broussard, S. M. Clayton, S. A. Currie, E. B. Dees, X. Ding, E. M. Engel, D. E. Fellers, W. Fox, P. Geltenbort, K. P. Hickerson, M. A. Hoffbauer, A. T. Holley, A. Komives, C.-Y. Liu, S. W. T. MacDonald, M. Makela, C. L. Morris, J. D. Ortiz, J. Ramsey, D. J. Salvat, A. Saunders, S. J. Seestrom, E. I. Sharapov, S. K. Sjue, Z. Tang, J. Vanderwerp, B. Vogelaar, P. L. Walstrom, Z. Wang, W. Wei, H. L. Weaver, J. W. Wexler, T. L. Womack, A. R. Young and B. A. Zeck

Science **360** (6389), 627-632.
DOI: 10.1126/science.aan8895originally published online May 6, 2018

How long does a neutron live?

Unlike the proton, whose lifetime is longer than the age of the universe, a free neutron decays with a lifetime of about 15 minutes. Measuring the exact lifetime of neutrons is surprisingly tricky; putting them in a container and monitoring their decay can lead to errors because some neutrons will be lost owing to interactions with the container walls. To overcome this problem, Pattie *et al.* measured the lifetime in a trap where ultracold polarized neutrons were levitated by magnetic fields, precluding interactions with the trap walls (see the Perspective by Mumm). This more precise determination of the neutron lifetime will aid our understanding of how the first nuclei formed after the Big Bang.

Science, this issue p. 627; see also p. 605

ARTICLE TOOLS	http://science.sciencemag.org/content/360/6389/627
SUPPLEMENTARY MATERIALS	http://science.sciencemag.org/content/suppl/2018/05/04/science.aan8895.DC1
RELATED CONTENT	http://science.sciencemag.org/content/sci/360/6389/605.full
REFERENCES	This article cites 22 articles, 0 of which you can access for free http://science.sciencemag.org/content/360/6389/627#BIBL
PERMISSIONS	http://www.sciencemag.org/help/reprints-and-permissions

Use of this article is subject to the Terms of Service

Science (print ISSN 0036-8075; online ISSN 1095-9203) is published by the American Association for the Advancement of Science, 1200 New York Avenue NW, Washington, DC 20005. 2017 © The Authors, some rights reserved; exclusive licensee American Association for the Advancement of Science. No claim to original U.S. Government Works. The title *Science* is a registered trademark of AAAS.

Downloaded from http://science.sciencemag.org/ on May 10, 2018